

Cite this article

Faleschini F, Trento D, Lopez VO and Zanini MA
Shear transfer in fly ash concrete with electric arc furnace aggregates.
Magazine of Concrete Research,
<https://doi.org/10.1680/jmacr.22.00280>

Research Article

Paper 2200280
Received 28/09/2022;
Accepted 24/02/2023

ICE Publishing: All rights reserved

Shear transfer in fly ash concrete with electric arc furnace aggregates

Flora Faleschini

Department of Civil, Environmental and Architectural Engineering,
University of Padova, Padova, Italy; Department of Industrial Engineering,
University of Padova, Padova, Italy (corresponding author:
flora.faleschini@dicea.unipd.it)

Daniel Trento

Department of Civil, Environmental and Architectural Engineering,
University of Padova, Padova, Italy

Vanesa-Ortega Lopez

Department of Civil Engineering, Escuela Politécnica Superior, University of
Burgos, Burgos, Spain

Mariano Angelo Zanini

Department of Civil, Environmental and Architectural Engineering,
University of Padova, Padova, Italy

The friction shear behaviour of concrete containing electric arc furnace (EAF) slag (hereafter called EAFC) was experimentally evaluated and compared with a reference counterpart made with only natural aggregates. Two concrete mixes were cast, both containing a cement blended with 30% fly ash to improve their sustainability. For each mix, other than analysing the main mechanical properties (compressive strength, tensile strength and elastic modulus), push-off specimens were tested to determine the shear strength, failure modes, stress–slip and stress–crack opening curves. There was a clearly enhancement in the shear strength of EAFC compared with the reference concrete, even though the relations between shear strength and tensile strength were similar for the two concretes. The results were also compared with data from the literature pertaining to ordinary concrete and recycled aggregate concrete. Existing models from both design codes and the literature were applied to the experimental results and conservative predictions were obtained in all cases. The safety margin for the EAFC was found to be higher than that for the reference concrete.

Q1 **Keywords:** EAFC/mechanical properties/push-off/recycled concrete/shear strength

Q2 Notation

A_c	shear plane area
A_{sw}	transverse steel area
c	cohesion
D_1, D_2	recorded displacements
E_c	elastic modulus
E_{cm}	average elastic modulus
d_s	steel bar diameter
f_c	compressive strength
f_{ck}	characteristic compressive strength at 28 days
f_{cm}	average compressive strength at 28 days
f_{ct}	indirect tensile strength
f_{ctd}	design tensile strength
f_{ctk}	characteristic tensile strength
f_{ctm}	average tensile strength
P_u	ultimate load
s	relative vertical slip
s_u	ultimate slip
w_u	average ultimate crack width
μ	coefficient of friction
ρ_c	fresh density
ρ_v	volumetric transverse reinforcement ratio
Q3 σ_{ncr}	stress normal to the shear plane
τ	shear stress
τ_u	ultimate shear strength
τ_u^*, τ_u^+	dimensionless shear strengths (shear strengths divided by $f_c^{1/2}$ and f_{ct} , respectively)

Introduction

Shear failure is considered to be one the most dangerous types of failure in reinforced concrete (RC) structures as it occurs suddenly, without warning cracks. Because of this brittle failure, shear transfer mechanisms have been studied widely in the literature in order to evaluate how concrete properties and steel arrangements influence shear transfer along a sliding plane. Among the different effects that play a role in the shear strength of RC members, aggregate interlock is worthy of mention. According to the first models proposed by Walraven (1981) and Paulay and Loeber (1974), this phenomenon develops when aggregates at one side of a crack come into contact with the cementing matrix on the other side, giving rise to tangential frictional stresses. Thus, aggregate interlock depends significantly on the crack opening, slip and, at a more in-depth level, on the aggregates' morphology (i.e. roughness, shape and size) (Ruiz *et al.*, 2015). In this context, the work of Sagasetta and Vollum (2011) is noteworthy: the authors identified that even the mineralogic composition of the aggregate has an impact on shear strength transfer along cracks and experimentally observed differences between limestone and dredged marine gravel. They noted different brittleness of the aggregates, which affected the crack paths, but similar aggregate dilatancy values were observed. The strength of the cementitious matrix also positively influences the shear strength (Fenwick and Paulay, 1968), as does the presence of confining pressure (Hobbs, 1974).

PROOFS

Several experimental methods can be used to investigate shear strength directly, but the most well known is the testing of push-off specimens (Mattock and Hawkins, 1972). Figure 1 shows test layouts that can be used to investigate shear transfer mechanisms on Z-type push-off specimens (Soetens and Matthys, 2017) (Figure 1(a)), single-notched FIP-type specimens (FIP, 1978) (Figure 1(b)) and double-notched push-through specimens or modified JCSE SF6 specimens (Cuenca *et al.*, 2020) (Figure 1(c)). Variations may exist, depending on the specific problem to be analysed, such as possible pre-cracking, the arrangement of steel reinforcement, specimen dimensions, the presence of confinement and so on. The push-off test method shown in Figure 1(a) allows the application of shear stress along a prescribed sliding plane, which is identified through cut or cast notches in the specimen. This typically ensures the most representative results, although it is more difficult to execute than the other layouts. The push-off specimen is made from two L-shaped blocks, connected together by a transverse element in the middle of the specimen. Load is applied on the top surface, resulting in direct shear along the plane that connects the two edges of the notches (dashed red line in Figure 1(a)). The main advantage of adopting this test method is that the specimens have small dimensions and the shear sliding plane can be identified easily: in this way it is possible to carry out many experimental tests to address the specific influence of the analysed variable, which is clearly difficult to manage when testing real-scale elements. Additionally, when testing RC beams failing in shear, the interaction with bending actions is clearly not negligible.

In this context, the development of new, sustainable concretes in which natural aggregate (NA) is replaced with recycled aggregate (RA) opens questions about how the aggregate substitution influences the shear strength of RC elements and, importantly, how it impacts on the aggregate interlock shear

transfer mechanism. Several research groups have attempted to provide answers to these questions, depending on additions to the concrete mix or on the recycled material used as an aggregate substitution.

In the first group, it is worth mentioning the works carried out on fibre-reinforced concrete, where dispersed fibres added to the matrix carry a significant portion of the shear stresses (Barr, 1987; Minelli and Plizzari, 2013). Experimental results of push-off specimens (Barragan *et al.*, 2006) and modified push-off specimens (Echegaray-Oviedo *et al.*, 2017) have clearly demonstrated the crack bridging ability of steel fibres in samples subjected to a combination of both mode I (opening) and mode II (sliding) crack propagation, and this has also been confirmed in modified JCSE SF6 specimens (Soetens and Matthys, 2017).

With regard to the second group of works, research has been conducted to study the influence of the introduction of recycled materials on concrete shear strength. However, only a few studies were carried out under pure shear failure. Fonteboa *et al.* (2010) investigated the shear strength of recycled aggregate concrete (RAC); they observed a reduction in shear friction capacity, especially for specimens designed without transverse reinforcement. Xiao *et al.* (2012) obtained the same results and identified the cause of strength loss as the presence of microcracks and internal damage to the attached mortar of the RA. Fakitsas *et al.* (2012) confirmed these observations and showed that the shear planes in high-strength concrete made with RA go through the aggregates, rather than around them, thus reducing the shear strength. In normal-strength concrete, Rahal and Hassan (2021) demonstrated that the failure surfaces in RAC were generally less rough than those in natural aggregate concrete (NAC) due to the development of cracks along the old interfacial transition zone (ITZ) of the

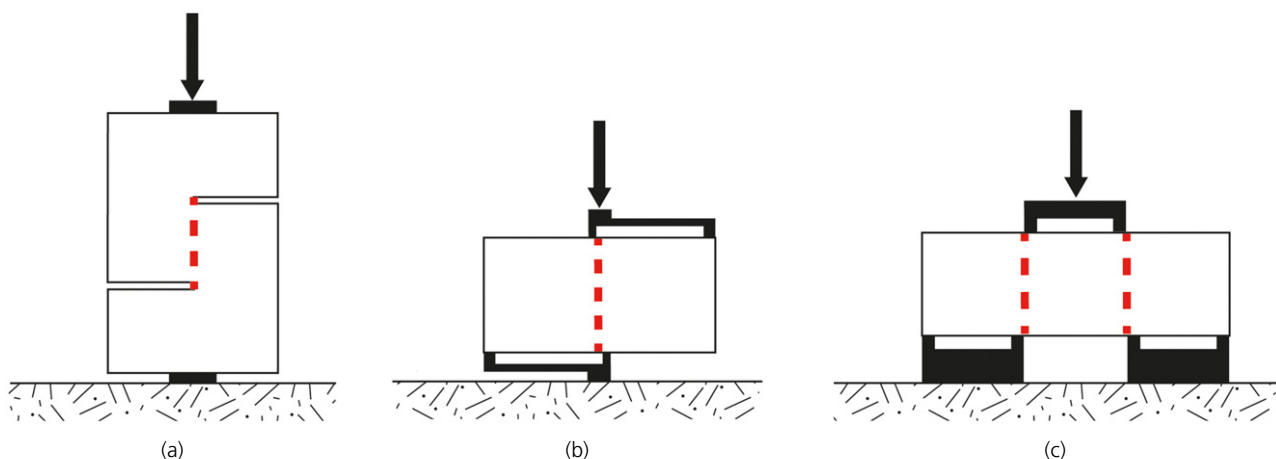


Figure 1. Layouts used to investigate shear transfer mechanisms: (a) push-off specimen; (b) FIP specimen; (c) modified JSCE SF6 specimen

PROOFS

RA, this being weaker than the new cementitious matrix. However, when confined, the shear strength improves substantially, as numerically validated by Sun *et al.* (2018). This is due to the effect of the compression force applied normally to the interface, which increases the contribution of aggregate interlock and friction, in the same way in RAC and NAC. Waseem and Singh (2016) studied the shear stress–slip relationships of RAC compared with NAC in push-off specimens transversally reinforced with stirrups and without. When reinforcement was present and it crossed the shear interface, clamping and dowel actions affected the shear strength development significantly. Waseem and Singh (2016) also applied some existing strength prediction models, with acceptable results. Trindade *et al.* (2020) and Rahal and Al-Khaleefi (2015) obtained a conservative prediction of the shear strength when ACI 318-19 (ACI, 2019), even though the shear strength of RAC is inferior to that of NAC; however, unconservative predictions were obtained with other formulas. More recent works have attempted to study the interaction of RAC with steel fibres (Gao *et al.*, 2017) and the direct shear strength of other concrete types (e.g. with alkali-activated slag) (Manjunath *et al.*, 2020).

According to the best knowledge of the authors, no specific studies have been carried out to investigate shear transfer in concrete made with electric arc furnace (EAF) slag (hereafter called EAFC). This kind of sustainable concrete is realised by substituting NA with EAF slag, which is a very hard, black, stone-like, recycled material from the steelmaking industry (Figure 2). Several works in the literature have shown that, compared with NAC, EAFC has similar or even superior mechanical properties (Abu-Eishah *et al.*, 2012; Arribas *et al.*, 2015; Monosi *et al.*, 2016), especially when the EAF slag used is in the coarse grading fraction (Faleschini *et al.*, 2015). Promising results have been obtained for the use of EAFC for structural applications, as observed from tests on different real-scale elements: RC beams under flexure–shear (Faleschini and Pellegrino, 2013; Santamaría *et al.*, 2021), RC columns under axial loading (Lee *et al.*, 2018) and RC beam–column joints under cyclic reversed lateral loading with flexural–shear failure (Faleschini *et al.*, 2017a). Furthermore, some recent works have highlighted that, under gravity load (Zanini, 2019) and seismic excitation (Faleschini *et al.*, 2019), the use of EAFC provides the same, or even higher, structural reliability than NAC. However, for proper interpretation of the shear capacity of this kind of concrete and its further safe use in RC structures, an experimental programme aimed at assessing the aggregate interlock and friction contribution to shear strength is required – this is the topic covered in this work.

Results are provided for the specific case of a sustainable EAFC mix designed with 100% coarse EAF aggregates (as a replacement for natural gravel) and with cement blended with 30% fly ash. Plain un-notched push-off specimens without transverse reinforcement were tested in order to compare the



Figure 2. EAF slag of different particle size

results with data from the literature on specimens with similar geometry and steel reinforcement, but made with RAC. The suitability of some current models from the literature and existing codes to predict the basic mechanical properties and shear strength of EAFC was evaluated. This was carried out in order to evaluate if the same accuracy could be obtained using these models originally developed for NAC mixes.

Experimental programme

Materials and mix design

NAC and EAFC mixes were designed: the former contained only NA, whereas EAF slag was used in place of natural gravel in the latter. The fine aggregate (river sand) fraction (0–4 mm) was the same for both mixes. The physical properties of the aggregates are provided in Table 1. The aggregate grading curves are shown in Figure 3: note that three fractions of EAF slag were used to replace the 4–16 mm NA fraction, in different proportions. All the mixes were made using Cem IV/A (V) 42.5 R cement, according to BS EN 197-1:2011 (BSI, 2011). Adopting a pozzolanic cement with about 30% fly ash replacing the clinker led to a more sustainable mix, with a lower carbon dioxide footprint than concrete made with Portland cement and a more rapid strength gain. A similar cement type (Cem IV/B), containing much larger quantities of supplementary cementitious materials (SCMs), was used by Santamaría *et al.* (2020) in combination with EAF slag.

PROOFS

Table 1. Physical properties of aggregates

	NA (0–4 mm)	NA (4–16 mm)	EAF slag (4–8 mm)	EAF slag (8–12 mm)	EAF slag (8–16 mm)
Density (saturated surface-dry): kg/m ³	2644	2769	3840	3800	3784
Water absorption 24 h: %	2.71	1.37	0.89	1.01	0.82
Shape	Round	Round	Sharp	Sharp	Sharp

Q34

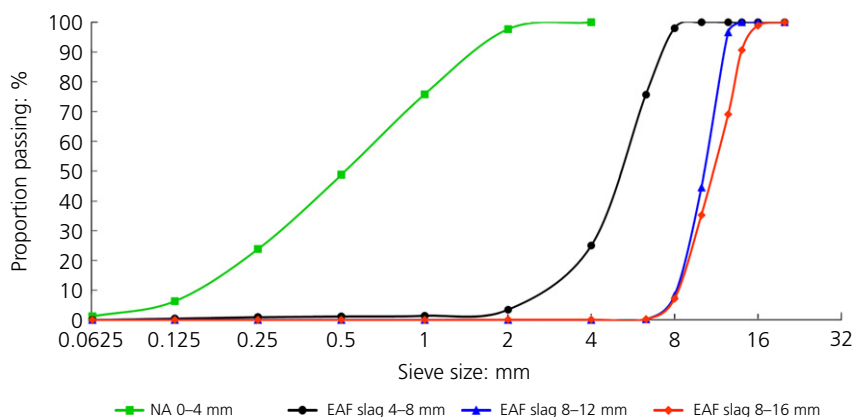


Figure 3. Grading curves of aggregates

However, the experience of those authors was not positive as undesirable thixotropic phenomena occurred both in pumpable and self-compacting mixes, leading to a non-satisfactory combination of the two materials. In the current work, an attempt to use the two materials synergistically was made, assuming that less SCM in the blended cement would not affect the workability of the mix. Tap water from the city of Padova, Italy, which does not contain any harmful substances, was used for mixing. A superplasticising sulfonated naphthalene admixture was added at different percentages of cement weight to reach the required consistency.

Table 2 shows the mix design of the two concretes. For each mix, three push-off specimens were cast, along with two cylinders ($\varnothing 100 \times 200$ mm) for each property to evaluate the compressive strength (f_c) at 14, 28 and 56 days and the indirect tensile strength (f_{ct}) and elastic modulus (E_c) at 28 days. The number of samples fabricated was limited due to the small capacity of the mixer. After casting, all the samples were covered with humid fabric and sealed in plastic bags for 24 h. They were then demoulded and cured in water ($20 \pm 1^\circ\text{C}$) until the test ages.

Push-off specimens and test setup

The push-off test method was adopted to study the shear transfer mechanism in EAFC. The geometry and reinforcement details of the push-off specimens are shown in Figure 4. The geometry was similar to that used in other studies (Mathews *et al.*, 2021; Rahal and Al-Khaleefi, 2015). The height of each specimen was

Table 2. Concrete mix designs

	NAC	EAFC
Cem IV/A (V) 42.5 R: kg/m ³	400	400
Water: kg/m ³	200	200
w/c	0.5	0.5
NA (0–4 mm): kg/m ³	862.5	862.5
NA (4–16 mm): kg/m ³	1026.5	—
EAF slag (4–8 mm): kg/m ³	—	501.9
EAF slag (8–12 mm): kg/m ³	—	358.6
EAF slag (8–16 mm): kg/m ³	—	563.0
Superplasticiser: kg/m ³	3.2	4.8

Q35

260 mm, with a rectangular cross-section of $b \times h = 140 \times 100$ mm. The specimens had two intermediate notches, directly realised due to the shape of the formwork, which allowed control of the flow of stresses and aimed to concentrate the development of shear stresses properly across the plane of contact between the two halves of each specimen. This region of the specimen is the shear transfer plane, where both shear and normal stresses act simultaneously. Four deformed L-shaped longitudinal bars of 10 mm diameter were located in the specimens to prevent possible flexural failure outside the investigated shear plane region; these were supported by six transverse bars of 6 mm diameter. Steel type B450C was used for both types of reinforcement (MIT, 2018). The main mechanical properties of the steel bars are shown in Table 3. No transverse reinforcement was present crossing the shear plane (similar to the work of Fonteboa *et al.* (2010)) for the condition of $\rho_v = A_{sw}/A_c = 0$, where A_{sw} is the transverse

PROOFS

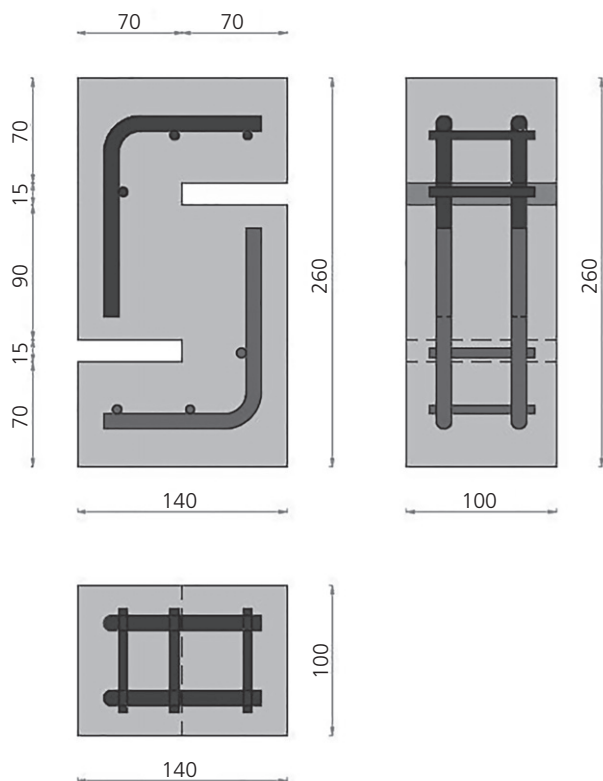


Figure 4. Push-off specimens: geometry and reinforcement details (dimensions in mm)

Table 3. Steel bar properties (average of three samples per each bar diameter (d_s))

	$d_s = 10$ mm	$d_s = 6$ mm
Tensile yield strength: MPa	545.8	515.7
Ultimate strength: MPa	679.8	602.1
Yield strain: %	0.32	0.31
Ultimate strain: %	9.67	9.79

steel area, A_c is the concrete area in the sliding plane and ρ_v is the volumetric transverse reinforcement ratio. The same configuration was used by Barragan *et al.* (2006), Mathews *et al.* (2021), Rahal and Al-Khaleefi (2015) and Waseem and Singh (2016). In this way, the pure effect of the friction contribution to the shear strength could be analysed, without focusing, at this stage, on the interaction with the reinforcement. In fact, it is worth recalling that non-ordinary concretes (e.g. concretes made with recycled or lightweight aggregates or high-strength concretes) are subject to different aggregate interlock mechanisms due to different crack kinematics (Fang *et al.*, 2020, Ruiz, 2021).

The specimens were loaded in a universal 600 kN capacity machine, with monotonic loading under displacement control, fixed at 0.3 mm/min, similar to that used by Yusuf *et al.* (2019). Figure 5 shows a push-off specimen before loading. The instrumentation included four linear voltage displacement transducers



Figure 5. Push-off test setup and instrumentation positions

(LVDTs) and two displacement and strain transducers (DSTs). A pair of LVDTs was used on two faces of the specimen and the displacement recorded by each instrument (D_1 and D_2) was used to calculate the relative vertical slip (s) between the two L-shaped halves:

$$1. \quad s_i = D_{1,i} - D_{2,i}$$

for each face (i) of the specimen. The precision of the LVDTs was ± 0.01 mm over a gauge length of 20 mm. The DSTs directly measured the crack opening in the transverse direction as they were placed crossing the shear plane, similarly to the work of da Cunha *et al.* (2022). The precision of the DSTs was ± 0.001 mm, with a maximum opening of 2.5 mm. In the loading machine, a hinge connection was present on the top of the actuator: the aim of this was to keep the applied load as axial as possible, thus minimising bending emerging from irregularities possibly present in the specimens and maintaining pure shear action in the analysed region of the specimen. With the same objective (i.e. to minimise the effect of discontinuities and irregularities on the surfaces), a restraining steel plate and a thin layer of high-strength mortar were placed on the top and bottom of the specimen.

Results

The results of the experimental campaign are now discussed in terms of the fresh behaviour and mechanical properties at 14, 28 and 56 days, the shear strength and failure mode of push-off specimens, the shear stress–slip curves and the shear stress–crack opening curves.

Fresh behaviour and concrete mechanical properties

The fresh and hardened properties of the concrete mixes (Abram's cone slump, average fresh density (ρ_c), hardened

PROOFS

density ($\rho_{c,28}$), compressive strength at 14, 28 and 56 days ($f_{c,14}$, $f_{c,28}$ and $f_{c,56}$), indirect tensile strength through splitting tests at 28 days ($f_{ct,28}$) and secant elastic modulus at 28 days ($E_{c,28}$) are shown in Table 4.

Santamaría *et al.* (2020) found that, when pozzolanic cement with a large amount of SCM (Cem IV/B) was used, a significant reduction in workability was experienced – such a large reduction that Santamaría *et al.* (2020) suggested that the combination of Cem IV/B and EAF slag is unsuitable. In the current work, the workability of the EAFC made with Cem IV/A (which differs from Cem IV/B by the amount of SCM) was sufficient and the fresh EAFC had the same slump class as the NAC mix (consistency class S3 according to BS EN 206-1:2014 (BSI, 2014)). Compared with the NAC, only a small reduction in the slump of the EAFC was found; this is due to the well-known shape effect of EAF slag, which makes fresh EAFC more difficult to place and work (Santamaría *et al.*, 2017). Typically, an adjustment of the content of fine particles in the mix is sufficient to prevent this phenomenon. Furthermore, during the casting operations, no sudden workability loss was experienced, thus proving the feasibility of combining slag aggregates with pozzolanic cement, at least from the point of view of workability.

Concerning the mechanical properties, the results obtained confirm the current knowledge about EAFC. In this work, compared with the NAC, the EAFC showed compressive strength increases of about 44%, 37% and 34% after 14, 28 and 56 days of curing, respectively. The increases in tensile strength and elastic modulus were 28% and 36%, respectively. These results confirm the good interaction of the EAF slag with the blended

cement, which yielded a more rapid strength gain than that of the NAC and continuous later strength development, as shown by the results after 56 days of curing. The strength enhancement compared with NAC has been already explained in the literature as a consequence of the intrinsic greater strength of EAF aggregates compared with NA (linked to the high content of iron oxides (Roslan *et al.*, 2020)), the good adhesion between the slag and cementitious matrix due to the effect of the shape of the EAF slag (Tamayo *et al.*, 2019) and the high quality of the ITZ, due to enrichment, in the aggregate wall zone, of products from the late hydration of the slag (Arribas *et al.*, 2015).

Assessment of mechanical properties based on code predictions

Table 5 shows comparisons of the experimentally obtained mean concrete tensile strengths and elastic moduli with those predicted using the formulas of ACI 318-19 (ACI, 2019) and BS EN 1992-1-1:2004 (henceforth referred to as EC2) (BSI, 2004). It is worth recalling that, very often, only the compressive strength is experimentally investigated to characterise the quality of a concrete mix; other mechanical properties are only seldom tested in practice. The indirect tensile strength (f_{ct}) is often expressed as a power of the compressive strength. According to ACI (2019) and BSI (2004), the average tensile strength (at 28 days) can be estimated using Equations 2 and 3, respectively.

$$2. \quad f_{ctm} = 0.56\sqrt{f_{cm}}$$

$$3. \quad \begin{aligned} f_{ctm} &= 0.3(f_{ck})^{2/3} & f_{ck} < 50 \\ f_{ctm} &= 2.12 \times \ln(1 + 0.1f_{cm}) & f_{ck} \geq 50 \end{aligned}$$

f_{ck} and f_{cm} are, respectively, the characteristic and average compressive strength at 28 days, which are linked, in a simplified approach, by:

$$4. \quad f_{ck} = f_{cm} - 8 \text{ MPa}$$

The values of f_{ctm} estimated using Equations 2 and 3 differed from the experimental values by 2% and 17% respectively for

Table 4. Fresh and hardened concrete properties

	NAC	EAFC
Slump: cm	12.0	10.0
ρ_c : kg/m ³	2407	2824
$\rho_{c,28}$: kg/m ³	2431	2828
$f_{c,14}$: MPa	32.48	46.98
$f_{c,28}$: MPa	38.96	53.34
$f_{c,56}$: MPa	43.89	58.81
$f_{ct,28}$: MPa	3.56	4.56
$E_{c,28}$: GPa	28.142	38.289

Table 5. Experimental and predicted mechanical properties

	f_{ctm} : MPa			E_{cm} : GPa		
	Exp.	ACI 318-19 (ACI, 2019)	EC2 (BSI, 2004)	Exp.	ACI 318-19 (ACI, 2019)	EC2 (BSI, 2004)
NAC	3.56	3.50	2.96	28.142	29.336	33.083
EAFC	4.56	4.09	3.81	38.289	34.326	36.356 (38.170 ^a)

^aApplying a density-correction factor for EAF aggregates

PROOFS

the NAC and by 11% and 17% respectively for the EAFC. Both equations underestimated f_{ctm} , regardless of the mix, but the prediction of the ACI method was more accurate than that of EC2. However, the error of the EC2 method was constant for the two mixes (17%), whereas the error using ACI 318-19 changed significantly, with an error of 2% (i.e. almost precise) for the NAC and 11% for the EAFC. This is because these formulas were both calibrated on ordinary concretes and the EC2 method uses the characteristic value instead of the average value for the compressive strength, thus being implicitly more conservative.

The average elastic modulus E_{cm} (at 28 days) can also be estimated as a power function of the compressive strength, according to ACI 318-19 (ACI, 2019) and EC2 (BSI, 2004) as Equations 5 and 6, respectively.

$$5. \quad E_{cm} = 4700\sqrt{f_{cm}}$$

$$6. \quad E_{cm} = 22000\left(\frac{f_{cm}}{10}\right)^{0.3}$$

Equations 5 and 6 both overestimated E_{cm} for the NAC mix (by 4% and 17%, respectively), whereas they underestimated it for the EAFC (by -10% and -5%, respectively). It is worth noting that the EC2 method allows for a correction of the predicted value depending on the aggregate type, which can be considered as a density-correction factor. In particular, for basalt aggregates, E_{cm} should be increased by 20%; in the case of other lightweight aggregates, a reduction of 10–20% is applied. Other works have shown that the inclusion of such a modification improves the estimation of E_{cm} compared with other codes, especially for those concretes with lightweight or heavy-weight aggregates (Revilla-Cuesta *et al.*, 2022). As such, applying a correction of +5% for the EAF aggregates, the prediction showed very high accuracy (an error of less than 1%).

Main results of shear transfer tests

The main test results of the experimental campaign are provided in Table 6. The table lists the ultimate loads (P_u), the ultimate shear strengths (τ_u), evaluated as P_u/A_c , where A_c is the shear plane area (here, 9000 mm²), the average ultimate slips (s_u), evaluated at P_u and the average ultimate crack widths (w_u), evaluated at P_u . Results are shown for each tested specimen, along with the averages and standard deviations (SDs).

Shear strength and failure mode

As shown in Table 6, the shear strength of the EAFC was higher than that of the NAC (average increase of 30%). The results showed almost the same scatter, as proved by the similar SDs and the same coefficient of variation (CoV) (CoV = SD/average = 0.10 in both cases). This result is a

Table 6. Main results of push-off tests

	P_u : kN	τ_u : MPa	s_u : mm	w_u : mm
NAC				
NAC-1	54.98	6.11	0.511	0.054
NAC-2	46.44	5.16	0.303	0.025
NAC-3	57.00	6.33	0.466	0.037
Average	52.81	5.86	0.427	0.039
SD	5.61	0.62	0.109	0.015
EAFC				
EAFC-1	70.37	7.82	0.316	0.026
EAFC-2	60.98	6.78	0.248	—
EAFC-3	73.80	8.20	0.393	0.050
Average	68.38	7.60	0.319	0.038
SD	6.64	0.74	0.073	0.017

fundamental point for ensuring the widespread use of EAFC for structural applications, because it means that the heterogeneity possibly present in a recycled material does not substantially affect the homogeneity of concrete properties.

The shear strengths were divided by $f_c^{1/2}$ and f_{ct} to obtain τ_u^* and τ_u^+ , respectively. Several works have reported a clear effect of concrete mechanical properties on the shear strength, typically dependent on $f_c^{1/2}$ (Rahal *et al.*, 2016), which is a simplified way of defining f_{ct} , according to ACI 318-19 (ACI, 2019). However, as noted earlier in the paper, when dealing with non-conventional concretes, the relation between f_c and f_{ct} might not follow the same laws for NAC: in fact, the accuracy of the prediction of f_{ct} depending on $f_c^{1/2}$ (Equation 2) changes significantly for NAC and EAFC. This result depends on the interaction of EAF slag with the cementitious matrix, which properly modifies the interface characteristics, the thickness of the ITZ and the adhesion strength. Such evidence was also discussed by Faleschini *et al.* (2017b), when dealing with the bond of EAFC with steel rebars.

The dimensionless shear strengths (τ_u^* and τ_u^+) are listed in Table 7: both τ_u^* and τ_u^+ were higher for the EAFC than for the NAC. The average increase in τ_u^* for the EAFC was about 10%, which indicates that the enhanced mechanical properties due to the use of EAF slag in place of NA contributed substantially to the shear strength enhancement. The increase in τ_u^+ for the EAFC compared with the value for the NAC was marginal (only 1%). In other words, both mixes had practically the same τ_u^+ , which indicates that the splitting tensile strength was well correlated with the shear strength. Apart from the increased strength of the EAF slag, the enhancement in EAFC shear strength may thus be attributed to the sharp shape of the EAF aggregates, which would affect the tensile behaviour of the concrete, allow contact areas to be developed and increase the friction between the two L-shaped blocks, consistent with the findings of Yang *et al.* (2017).

Concerning the failure modes, Figure 6 shows images of representative specimens of NAC and EAFC after testing. When loaded, the specimens did not display any visible cracking

PROOFS

Table 7. Dimensionless shear strengths

	τ_u^*	τ_u^+
NAC		
NAC-1	0.98	1.72
NAC-2	0.83	1.45
NAC-3	1.01	1.78
Average	0.94	1.65
SD	0.10	0.17
EAFC		
EAFC-1	1.07	1.71
EAFC-2	0.93	1.49
EAFC-3	1.23	1.80
Average	1.04	1.67
SD	0.10	0.16

phenomena until more the 90% of the peak load; only when approaching the maximum applied load did some cracks start to open. Failure occurred in a brittle way, with the sudden formation of a first thick vertical crack and then sub-vertical cracks, crossing the shear plane and identifying a compressed strut. The first crack, which was the thickest, appeared first at one notch edge and was typically vertical; once the crack reached the second notch edge, the second main sub-vertical crack grew rapidly until failure. These cracks were inclined at a maximum of 30° from the shear plane. The failure mode was dominated by tensile splitting. The absence of any transverse reinforcement crossing the shear plane did not allow for a certain load after the peak load, resulting in a definitive separation between the two L-shaped blocks forming the push-off specimen. The same applied to the slip: initially, no clear slip was evident. Instead, the observed movement was linked more to a relative rotation between the two blocks due to the compression of the formed inclined concrete strut. For the sake of brevity, in this paper, this displacement is also referred to as slip. After this, a sudden increase in slip occurred, resulting in extensive separation of the two L-shaped blocks.

Figure 7 shows the split surfaces of NAC and EAFC specimens after testing. In both figures, it is possible to distinguish two phenomena when an aggregate is present in the shear surface: cracks passing directly through the aggregates, thus cutting the sample into two separate portions (Figure 8(a)), and cracks propagating around the aggregates, concentrated in the ITZ (Figure 8(b)). Both phenomena were present in the NAC and EAFC specimens, but with a main difference – in the EAFC, aggregate failure was dominant; in the NAC, the two cracking paths occurred with almost the same frequency. This behaviour was also confirmed from observations of the splitting surfaces after indirect tensile strength tests on the NAC and EAFC specimens. When analysing the crack paths, it should be noted that failure in the EAFC occurred at a load about 29% higher than that in the NAC and the cementitious matrix was of relatively good quality as the cement dosage was quite high. It can thus be stated that the good quality of the ITZ of the EAFC allowed one type of failure to be postponed

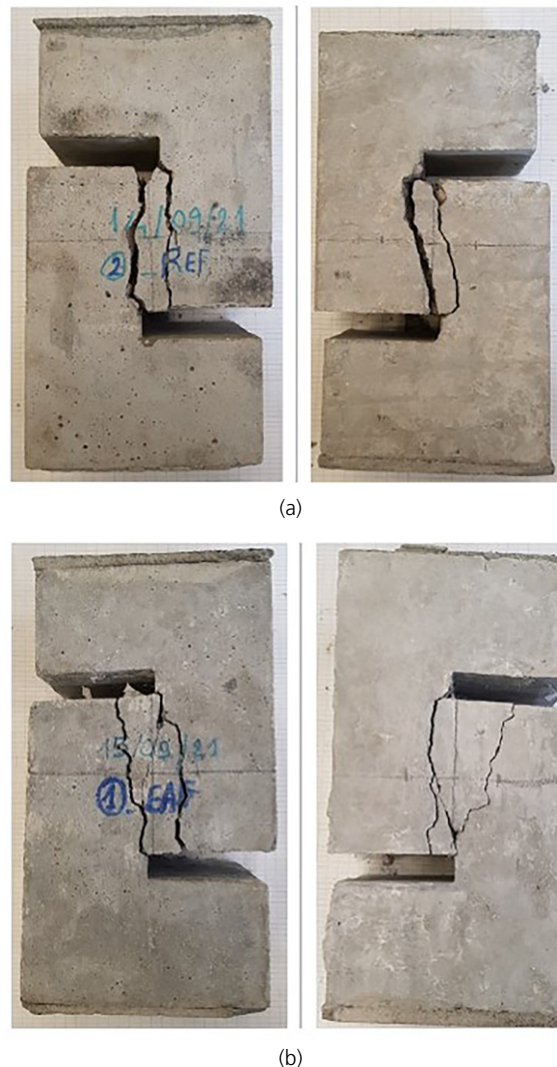


Figure 6. Failure modes and cracks in front and back faces of (a) NAC-2 and (b) EAFC-1

but, when the shear stress exceeded a certain limit, the specimens failed due to aggregate cracking (Figure 8(b)), as happens in high-strength concretes. The bond strength between the matrix and the slag should thus be similar to (or even higher than) the tensile strength of the EAF aggregate particles. Compared with the NAC, both the bond strengths and tensile strengths were higher in the EAFC. Furthermore, the crack surfaces exhibited significant angularities and roughness, allowing a certain contact area to develop.

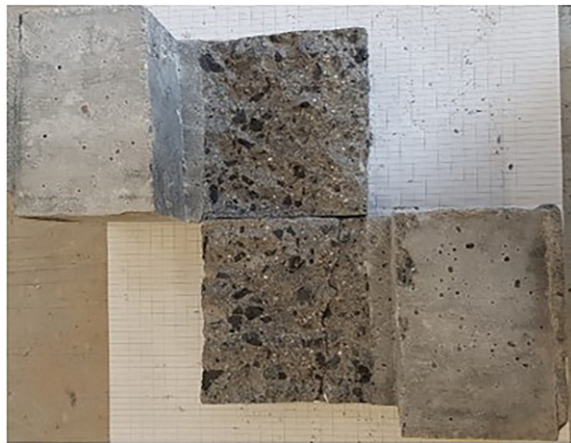
Shear stress–slip curves

The shear stress–slip curves of the NAC and EAFC specimens are plotted in Figure 9; the values were obtained as the average from the four LVDTs used on each specimen. Curves could be plotted until the ultimate shear strength was reached, beyond which the curves are interrupted due to the brittle failure of

PROOFS



(a)



(b)

Figure 7. Crack paths in the shear planes of (a) NAC-2 and (b) EAFC-1

the specimens. The maximum shear strength could not be maintained after the peak; the curves thus showed a sudden decrease, which are not shown here because of the few sense of slip records. The values of s_u listed in Table 6 were obtained from the shear stress–slip curves: the EAFC showed lower values of slip (on average 26% less than those of NAC). The CoV was similar for the two concrete types (0.26 for NAC and 0.22 for EAFC). These results indicate that the behaviour of EAFC was more brittle than the NAC: indeed, the brittleness of concrete increases with an increase in strength (Hamadi and Regan, 1980). This is confirmed by the slopes of the curves shown in Figure 9: the slope defines the shear stiffness, and the slope was greater for the EAFC than for the NAC. However, in general, the deformation behaviour of the two concrete types was similar.

Shear stress–crack opening curves

Shear stress–crack opening curves are plotted in Figure 10; the values were obtained as the average of the values from the

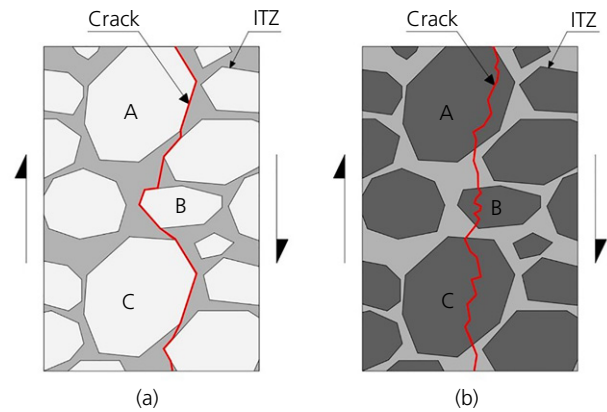


Figure 8. Shear cracks in plain concrete: (a) cracks around aggregate; (b) cracks through aggregate. A full-colour version of this figure can be found on the ICE Virtual Library (www.icevirtuallibrary.com)

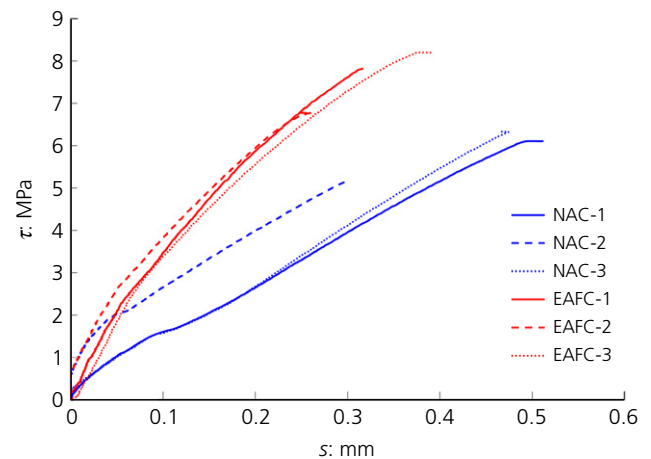


Figure 9. Shear stress–slip curves. A full-colour version of this figure can be found on the ICE Virtual Library (www.icevirtuallibrary.com)

two DSTs used on the two faces of each specimen. For specimen EAFC-2, it was not possible to provide the whole curve because cracks led to detachment of the instrumentation. All the other curves are plotted until the ultimate shear strength was reached, in a similarly way as for stress–slip curves. The values of ultimate crack width (w_u) listed in Table 6 were obtained from the curves shown in Figure 10. At shear stress peak, the NAC and EAFC were found to have almost the same average w_u (with a difference of only 2%). The w_u values were considerably low, in all cases less than 0.1 mm, consistent with the brittle failure mode. For both concrete mixes, the scatter of the results was similar and higher compared with the scatter of the other properties analysed. Indeed, the CoV was more than 35% for both the NAC and the EAFC.

PROOFS

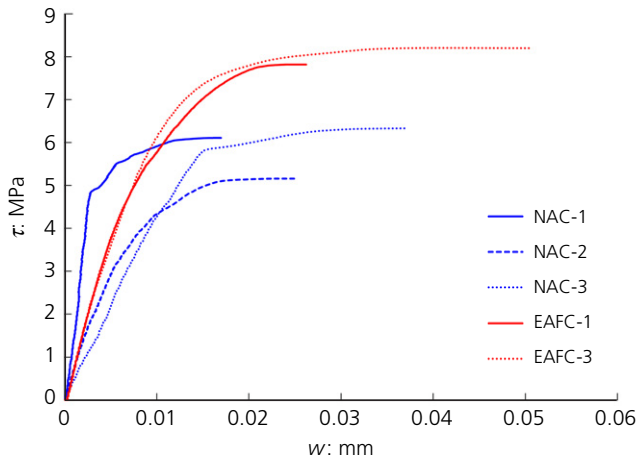


Figure 10. Shear stress–crack opening curves. A full-colour version of this figure can be found on the ICE Virtual Library (www.icevirtuallibrary.com)

Discussion

Comparison with literature data on NAC and RAC

In the literature, few works have reported on the shear transfer in concrete made with recycled constituents by means of push-off specimens and only some studies used specimens without any transverse reinforcement.

Fonteboa *et al.* (2010) studied the shear friction capacity of concretes containing recycled concrete aggregates (RCA) and silica fume using push-off specimens with $\rho_v = 0-0.57\%$. They tested four mixtures with a nominal cement dosage of 325 kg/m^3 and a water/cement ratio (w/c) of 0.55, with

specimens labelled as NAC, RAC, NACS and RACS. These specimens were, respectively, a conventional NAC, a mix with 50% RCA and NAC and RAC mixes with different contents of silica fume.

Waseem and Singh (2016) evaluated the shear transfer in normal- and high-strength RACs. They used different percentages of ρ_v to analyse the contribution of the stirrups. They cast three mixtures of normal concrete (nominal cement dosage of 435 kg/m^3 and $w/c = 0.45$) with RCA replacements ranging from 0 to 100% of the total coarse aggregate fraction (called N00, N50 and N100, respectively). The three mixtures were high-strength concretes (nominal cement dosage of 546 kg/m^3 and $w/c = 0.28$) with the same proportions of coarse aggregate fraction (called H00, H50 and H100, respectively).

Yusuf *et al.* (2019) analysed the shear transfer mechanisms in non-transversally reinforced NAC and RAC specimens, before and after high-temperature exposure. They used concrete mix designs similar to those used in this study (i.e. cement dosage of 416 kg/m^3 , $w/c = 0.52$ and a small amount of superplasticiser). The NA (crushed limestone) was substituted with different percentages of RA (0, 30, 70 and 100%); these mixes were called NAC, RAC30, RAC70 and RAC100, respectively. Since the mixtures cast by Yusuf *et al.* (2019) were similar to those of the current study in terms of mechanical strength at room temperature, the experimental results are suitable for comparison. However, unlike the NAC tested in the current work, Yusuf *et al.* (2019) used crushed aggregates (both natural and recycled), which in general ensures the development of a good friction mechanism during shear sliding because of the large contact areas between the particles and the matrix.

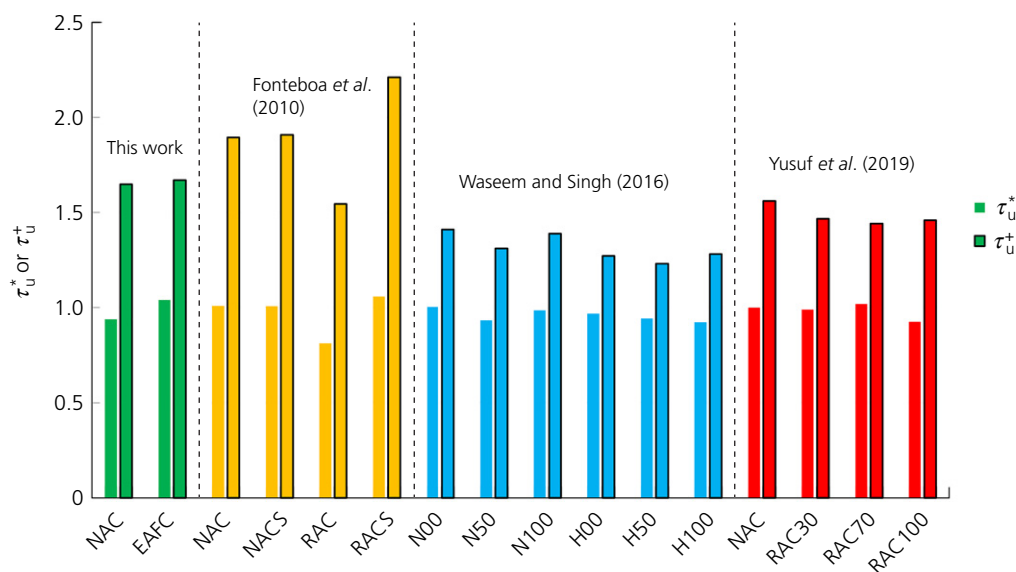


Figure 11. Comparison of dimensionless shear strengths of NAC, RAC and EAFC. A full-colour version of this figure can be found on the ICE Virtual Library (www.icevirtuallibrary.com)

PROOFS

Table 8. Predicted shear strengths from formulas based on the Coulomb failure criterion

Model and aggregate type	$\tau_u = c$	NAC		EAFC	
		$\tau_{u,th}$: MPa	$\Delta (= \tau_{u,th}/\tau_{u,exp})$	$\tau_{u,th}$: MPa	$\Delta (= \tau_{u,th}/\tau_{u,exp})$
Sagaseta and Vollum (2011)					
Gravel	$c = 0.57f_{ctk}$	2.029	0.346	2.599	0.342
Limestone	$c = 0.91f_{ctk}$	3.239	0.552	4.150	0.546
ACI 318-19 (ACI, 2019)					
Monolithic ordinary	$c = 2.75$ MPa	2.750	0.469	2.750	0.362
Rough ordinary	$c = 2.75$ MPa	2.750	0.469	2.750	0.362
Medium ordinary	—	—	—	—	—
EC2 (BSI, 2004)					
Rough surface	$c = 0.4f_{ctd}$	1.424	0.243	1.824	0.240
Smooth	$c = 0.2f_{ctd}$	0.712	0.121	0.912	0.120
Very smooth	$c = 0.025f_{ctd} - 0.1f_{ctd}$	0.356	0.061	0.456	0.060
Hamadi and Regan (1980)					
Gravel	$c = 4$ MPa	4.000	0.682	4.000	0.526
Expanded clay	$c = 2$ MPa	2.000	0.341	2.000	0.263
Climaco and Regan (2001)					
Rough	$c = 0.25f_c^{2/3}$	2.873	0.490	3.542	0.466
Medium	$c = 0.25f_c^{2/3}$	2.873	0.490	3.542	0.466
Smooth	$c = 0.5$ MPa	0.500	0.085	0.500	0.066

Figure 11 shows a comparison of the average normalised shear strengths (normalised to $f_c^{1/2}$ (τ_u^*) and f_{ct} (τ_u^+)) obtained in this work and the other studies. Overall, the results obtained in this work agree with those of NAC and RAC having a similar mix design and strength, with the EAFC in this work showing higher shear strength than most of the RAC counterparts. Only the mixes tested by Fonteboa *et al.* (2010) were characterised by higher normalised shear strength; this is because of the addition of silica fume, which was found to balance the loss of shear strength typically observed in RAC due to improvement of the cement matrix and thus the quality of the ITZ. The use of RA is almost always detrimental for shear strength development and also for other mechanical properties (Fakitsas *et al.*, 2012), because of the lower strength of RA compared with NA (Silva *et al.*, 2015). This is exactly the opposite of what happens in concretes cast with EAF slag as NA replacement: indeed, such a replacement is made with an aggregate generally characterised by remarkably higher strength than ordinary gravel. However, at failure, the cracks passed mainly through the EAF aggregates, opposite to that in NAC specimens where they passed both through the NAs and around them. The shear transfer capacity is thus higher in EAFC, thanks to a sort of interlocking at the macro-level, similarly to that reported by Sagaseta and Vollum (2011) and Haskett *et al.* (2011). Such phenomenon occurs due to the irregular shape of the crack surfaces, which allows contact areas to develop, despite the aggregate particle fracture almost completely at the cracks (compare Figures 7(a) and 7(b)).

Existing shear friction formulas

There are several formulas in the codes and the literature that can be used to estimate the shear transfer strength, mainly

developed for the verification of concrete construction joints. Most are based on the Coulomb failure criterion because, as the shear stress (τ) increases across an interface, most of the load is carried by the concrete-to-concrete cohesiveness:

$$7. \quad \tau = c + \mu\sigma_{ncr}$$

where c is the cohesion (typically, a percentage of the splitting tensile strength), μ is the coefficient of friction along the shear plane (depending on the roughness of the interface) and σ_{ncr} is the stress normal to the shear plane, which is connected to the amount of confinement provided by the transverse reinforcement crossing the shear plane.

When adopting Equation 7 for the case analysed in this work, the second term of the addition goes to zero because of the absence of transverse reinforcement. Thus, τ is constant and can be estimated according to the proposal of the single code/author, just depending on the crack surface roughness. All the formulas based on Equation 7 were developed primarily for ordinary concretes, where cracks do not directly cross aggregates but propagate around them. Only in a few cases have authors been more specific and proposed a particular value for different aggregate types (Climaco and Regan, 2001; Loov and Patnaik, 1994).


Table 8 lists some common expressions and values for estimating the shear strength under the testing conditions of this work, thus providing estimations of the experimental shear strengths. The table shows that the predictions are quite rough, generally underestimating by more than half the experimental values. In Table 8, the predictions that use f_{ctk} (the characteristic tensile strength) and f_{ctd} (the design tensile strength) were simplified here through the average tensile strength; thus, any partial safety factor was not

PROOFS

applied. Even with such a simplification, the predictions were far from the observed values, with the maximum $\Delta (= \tau_{u,th}/\tau_{u,exp})$ of 0.682, provided by the model of Hamadi and Regan (1980) model for gravel aggregates. The results were more conservative for the EAFC than for the NAC, thus the safety margin is even higher for the EAFC compared with the NAC, despite different cracking paths at the interface for the two concretes.

Conclusions

The effects of EAF slag as recycled coarse aggregate on the mechanical properties and shear strength of plain concrete were analysed experimentally in this work. Specifically, push-off specimens were tested to assess the shear transfer mechanisms. One novel element of this work is the synergistic adoption EAF slag and cement blended with fly ash, which produced a workable mix with good mechanical performance. The main conclusions on the shear strength of EAFC, about which no other experimental evidence in the literature was found, can be summarised as follows.

-  EAFC had higher shear strength than the NAC, as observed from push-off tests without transverse reinforcement or confinement effects. All the specimens failed in a brittle manner when the maximum load was reached. There was no difference in the global failure modes of the NAC and EAFC, although the crack paths along the interface differed.
- Two phenomena were distinguished when an aggregate was present in the shear surface: in the EAFC, for the cement dosage and w/c ratio used in this work, aggregate failure was dominant; in the NAC, the cracks mostly crossed the aggregates or propagated around them. However, the crack surfaces in the EAFC were very rough and presented many angularities, thus allowing for the development of several contact areas, increasing the shear strength thanks to macro-scale aggregate interlock.
- Existing shear friction formulas based on the Mohr–Coulomb approach, developed for ordinary concretes made with NA, were found to be very conservative for the analysed case, where only cohesiveness is accounted for. The formulas provided better predictions of the experimental values for the NAC than for the EAFC. However, the safety margin for the EAFC was higher than that for the NAC.

Acknowledgement

The authors would like to express their acknowledgement to Zerocento s.r.l. for providing the EAF slag.

REFERENCES

Abu-Eishah SI, El-Dieb AS and Bedir MS (2012) Performance of concrete mixtures made with electric arc furnace (EAF) steel slag aggregate produced in the Arabian Gulf region. *Construction and Building Materials* **34**: 249–256.

ACI (American Concrete Institute) (2019) ACI 318-19: Building code requirements for structural concrete and commentary on building code requirements for structural concrete. ACI, Farmington Hills, MI, USA.

Arribas I, Santamaria A, Ruiz E, Ortega-Lopez V and Manso JM (2015) Electric arc furnace slag and its use in hydraulic concrete. *Construction and Building Materials* **90**: 68–79.

Barr B (1987) *Fracture Characteristics of FRC Materials in Shear*. American Concrete Institute, Farmington Hills, MI, USA, ACI SP105-02, pp. 27–54.

Barragan B, Gettu R, Agullo L and Zerbino R (2006) Shear failure of steel fiber-reinforced concrete based on push-off tests. *ACI Materials Journal* **103(4)**: 251.

BSI (2004) BS EN 1992-1-1:2004: Eurocode 2: Design of concrete structures. BSI, London, UK.

BSI (2011) BS EN 197-1:2011: Cement – Composition, specifications and conformity criteria for common cements. BSI, London, UK.

BSI (2014) BS EN 206-1:2014: Concrete – Specification, performance, production and conformity. BSI, London, UK.

Climaco JCTS and Regan PE (2001) Evaluation of bond strength between old and new concrete in structural repairs. *Magazine of Concrete Research* **53(6)**: 377–390, <https://doi.org/10.1680/mac.2001.53.6.377>.

Cuenca E, Conforti A, Monfardini L and Minelli F (2020) Shear transfer across a crack in ordinary and alkali activated concrete reinforced by different fibre types. *Materials and Structures* **53(2)**: 1–15.

da Cunha BF, de Andrade Pinto RC and Savaris G (2022) Evaluation of self-consolidating concrete shear strength by means of push-off test. *Magazine of Concrete Research* **74(17)**: 897–888, <https://doi.org/10.1680/jmacr.21.00067>.

Echegaray-Oviedo J, Navarro-Gregori J, Cuenca E and Serna P (2017) Modified push-off test for analysing the shear behaviour of concrete cracks. *Strain* **53(6)**: e12239.

Fakitsas CG, Papakonstantinou PEA, Kioussis PD and Savva A (2012) Effects of recycled concrete aggregates on the compressive and shear strength of high-strength self-consolidating concrete. *Journal of Materials in Civil Engineering* **24(4)**: 356–361.

Faleschini F and Pellegrino C (2013) Experimental behavior of reinforced concrete beams with electric arc furnace slag as recycled aggregate. *ACI Materials Journal* **110**: 197–206.

Faleschini F, Fernández-Ruiz MA, Zanini MA et al. (2015) High performance concrete with electric arc furnace slag as aggregate: mechanical and durability properties. *Construction and Building Materials* **101**: 113–121.

Faleschini F, Hofer L, Zanini MA, dalla Benetta M and Pellegrino C (2017a) Experimental behavior of beam-column joints made with EAF concrete under cyclic loading. *Engineering Structures* **139**: 81–95.

Faleschini F, Santamaria A, Zanini MA, San Jose JT and Pellegrino C (2017b) Bond between steel reinforcement bars and electric arc furnace slag concrete. *Materials and Structures* **50(3)**: 1–13.

Faleschini F, Zanini MA and Toska K (2019) Seismic reliability assessment of code-conforming reinforced concrete buildings made with electric arc furnace slag aggregates. *Engineering Structures* **195**: 324–339.

Fang Z, Jiang H, Liu A, Feng J and Li Y (2020) Shear-friction behaviour on smooth interface between high-strength and lightweight concrete. *Magazine of Concrete Research* **72(2)**: 68–87, <https://doi.org/10.1680/jmacr.17.00393>.

Fenwick RC and Paulay T (1968) Mechanisms of shear resistance of concrete beams. *Journal of the Structural Division* **94(10)**: 2325–2350.

FIP (Federation Internationale de la Précontrainte) (1978) *Shear at the Interface of Precast and in Situ Concrete*. FIP, Lausanne, Switzerland.

Fonteboia BG, Martínez F, Carro D and Eiras J (2010) Shear friction capacity of recycled concretes. *Materiales de Construcción* **60(299)**: 53–67.

Q11

Q12

Q13

Q14

Q15

PROOFS

- Gao D, Zhang L and Nokken M (2017) Mechanical behavior of recycled coarse aggregate concrete reinforced with steel fibers under direct shear. *Cement & Concrete Composites* **79**: 1–8.
- Q16** Hamadi YD and Regan PE (1980) Behavior of normal and lightweight aggregate beams with shear cracks. *The Structural Engineer* **58B(4)**: 71–79.
- Haskett M, Oehlers DJ, Ali MSM and Sharma SK (2011) Evaluating the shear-friction resistance across sliding planes in concrete. *Engineering Structures* **33(4)**: 1357–1364.
- Hobbs DW (1974) *Strength and Deformation Properties of Plain Concrete Subject to Combined Stress. Part 3: Results Obtained on a Range of Flint Gravel aggregate Concretes*. Cement and Concrete Association, London, UK, Technical Report 42.497.
- Lee JM, Lee YJ, Jung YJ et al. (2018) Ductile capacity of reinforced concrete columns with electric arc furnace oxidizing slag aggregate. *Construction and Building Materials* **162**: 781–793.
- Q17** Loov RE and Patnaik AK (1994) Horizontal shear strength of composite concrete beams with a rough interface. *PCI Journal* **39(1)**: 48–69.
- Manjunath R, Narasimhan MC, Shashanka M, Vijayanand SD and Vinayaka J (2020) Experimental studies on shear strength characteristics of alkali activated slag concrete mixes. *Materials Today: Proceedings* **27**: 275–279.
- Q18** Mathews ME, Anand N, Lubl6y  and Kiran T (2021) Effect of elevated temperature on interfacial shear transfer capacity of self-compacting concrete. *Case Studies in Construction Materials* **15**: e00753.
- Q19** Mattock AH and Hawkins NM (1972) Shear transfer in reinforced concrete - recent research. *PCI Journal* **17(2)**: 55–75.
- Minelli F and Plizzari GA (2013) On the effectiveness of steel fibers as shear reinforcement. *ACI Structural Journal* **110(3)**: 379–390.
- Q20** MIT (Ministero delle Infrastrutture e dei Trasporti) (2018) Decreto 17 gennaio 2018. Aggiornamento delle «Norme tecniche per le costruzioni». MIT, Rome, Italy (in Italian).
- Monosi S, Ruello ML and Sani D (2016) Electric arc furnace slag as natural aggregate replacement in concrete production. *Cement & Concrete Composites* **66**: 66–72.
- Q21** Paulay T and Loeber PJ (1974) *Shear Transfer by Aggregate Interlock*. American Concrete Institute, Farmington Hills, MI, USA, ACI SP42, pp. 1–16.
- Rahal KN and Al-Khaleefi AL (2015) Shear-friction behavior of recycled and natural aggregate concrete-an experimental investigation. *ACI Structural Journal* **112(6)**: 725.
- Rahal KN and Hassan W (2021) Shear strength of plain concrete made of recycled low-strength concrete aggregates and natural aggregates. *Construction and Building Materials* **311**: 125317.
- Q22** Rahal KN, Khaleefi AL and Al-Sanee A (2016) An experimental investigation of shear-transfer strength of normal and high strength self compacting concrete. *Engineering Structures* **109**: 16–25.
- Q23** Revilla-Cuesta V, Faleschini F, Pellegrino C, Skaf M and Ortega-L6pez V (2022) Simultaneous addition of slag binder, recycled concrete aggregate and sustainable powders to self-compacting concrete: a synergistic mechanical-property approach. *Journal of Materials Research and Technology* **18**: 1886–1908.
- Q24** Roslan NH, Ismail M, Khalid NHA and Muhammad B (2020) Properties of concrete containing electric arc furnace steel slag and steel sludge. *Journal of Building Engineering* **28**: 101060.
- Q25** Ruiz MF (2021) The influence of the kinematics of rough surface engagement on the transfer of forces in cracked concrete. *Engineering Structures* **231**: 111650.
- Q26** Ruiz MF, Muttoni A and Sagaseta J (2015) Shear strength of concrete members without transverse reinforcement: a mechanical approach to consistently account for size and strain effects. *Engineering Structures* **99**: 360–372.
- Q27** Sagaseta J and Vollum RL (2011) Influence of aggregate fracture on shear transfer through cracks in reinforced concrete. *Magazine of Concrete Research* **63(2)**: 119–137, <https://doi.org/10.1680/macr.9.00191>.
- Santamara A, Orbe A, Losanez MM et al. (2017) Self-compacting concrete incorporating electric arc-furnace steelmaking slag as aggregate. *Materials & Design* **115**: 179–193.
- Q28** Santamara A, Ortega-L6pez V, Skaf M, Chica JA and Manso JM (2020) The study of properties and behavior of self-compacting concrete containing electric arc furnace slag (EAFS) as aggregate. *Ain Shams Engineering Journal* **11(1)**: 231–243.
- Santamara A, Romera JM, Marcos I, Revilla-Cuesta V and Ortega-L6pez V (2021) Shear strength assessment of reinforced concrete components containing EAF steel slag aggregates. *Journal of Building Engineering* **46**: 103730.
- Silva RV, de Brito J and Dhir RK (2015) Tensile strength behaviour of recycled aggregate concrete. *Construction and Building Materials* **83**: 108–118.
- Q29** Soetens T and Matthys S (2017) Shear-stress transfer across a crack in steel fibre-reinforced concrete. *Cement & Concrete Composites* **82**: 1–13.
- Q30** Sun C, Xiao J and Lange DA (2018) Simulation study on the shear transfer behavior of recycled aggregate concrete. *Structural Concrete* **19(1)**: 255–268.
- Tamayo P, Pacheco J, Thomas C, de Brito J and Rico J (2019) Mechanical and durability properties of concrete with coarse recycled aggregate produced with electric arc furnace slag concrete. *Applied Sciences* **10(1)**: 216.
- Trindade J, Garcia S and Fonseca G (2020) Experimental study of direct shear in concrete with recycled aggregate. *ACI Structural Journal* **117(5)**: 233–243.
- Walraven JC (1981) Fundamental analysis of aggregate interlock. *Journal of the Structural Division* **107(11)**: 2245–2270.
- Waseem SA and Singh B (2016) Shear transfer strength of normal and high-strength recycled aggregate concrete—an experimental investigation. *Construction and Building Materials* **125**: 29–40.
- Q31** Xiao J, Xie H and Yang Z (2012) Shear transfer across a crack in recycled aggregate concrete. *Cement and Concrete Research* **42(5)**: 700–709.
- Yang Y, Walraven J and Uijl JD (2017) Shear behavior of reinforced concrete beams without transverse reinforcement based on critical shear displacement. *Journal of Structural Engineering* **143(1)**: 04016146.
- Yusuf M, St-Onge P, Sarhat S and Green M (2019) Shear transfer strength of concrete made with recycled concrete aggregate after exposure to high temperatures. In *Proceedings of the 3rd International Fire Safety Symposium, Ottawa, Ontario, Canada*, pp. 305–314.
- Zanini MA (2019) Structural reliability of bridges realized with reinforced concretes containing electric arc furnace slag aggregates. *Engineering Structures* **188**: 305–319.
- Q33**

How can you contribute?

To discuss this paper, please submit up to 500 words to the editor at journals@ice.org.uk. Your contribution will be forwarded to the author(s) for a reply and, if considered appropriate by the editorial board, it will be published as a discussion in a future issue of the journal.

QUERY FORM

Institution of Civil Engineers (ICE)

Journal Title: **MAGAZINE OF CONCRETE RESEARCH (JMACR)**

Article No: **2200280**

AUTHOR: The following queries have arisen during the editing of your manuscript. Please answer the queries by making the requisite corrections at the appropriate positions in the text.

Query No.	Nature of Query	Author's Response
Q1	To improve your paper's discoverability on the ICE Virtual Library website, please select at least one additional keywords from the ICE Publishing keywords list (https://www.icevirtuallibrary.com/pb-assets/for%20authors/ICE%20Publishing%20keywords-1636044677.xlsx)	Please add: "Concrete technology & manufacture"
Q2	Notation list amended at copy-editing; please check all definitions are correct and add any missing definitions	OK.
Q3	'normal stress to the shear plane' changed to 'stress normal to the shear plane' : is this OK?	OK.
Q4	The reference citation 'Roslan, 2020' has been changed to 'Roslan <i>et al.</i> , 2020' with respect to the reference list provided; please check and confirm the change.	OK.
Q5	'first thick tension vertical' changed to 'first thick vertical crack': is this OK?	OK.
Q6	'ones the pattern achieves the second notch edge' changed to 'once the crack reached the second notch edge': OK?	OK.
Q7	'few sense of slip records': unsure what is meant here: please advise (few slip records??)	NO: "because slip records increased suddenly off scale, resulting in unreliable readings".
Q8	Is cross-ref to Figures 7(a) and 7(b) OK, or should this be Figures 8(a) and 8(b)?	IT IS "FIGURES 7A AND 7B".
Q9	'normal stress to the shear plane' changed to 'stress normal to the shear plane' : is this OK?	OK.
Q10	Please provide the issue number, if available, in Abu-Eishah <i>et al.</i> (2012).	The issue number is not provided.
Q11	Please provide the issue number, if available, in Arribas <i>et al.</i> (2015).	The issue number is not provided.
Q12	Please provide the issue number, if available, in Faleschini and Pellegrino (2013).	The issue number is "2".
Q13	Please provide the issue number, if available, in Faleschini <i>et al.</i> (2015).	The issue number is not provided.
Q14	Please provide the issue number, if available, in Faleschini <i>et al.</i> (2017a).	The issue number is not provided.
Q15	Please provide the issue number, if available, in Faleschini <i>et al.</i> (2019).	The issue number is not provided.
Q16	Please provide the issue number, if available, in Gao <i>et al.</i> (2017).	The issue number is not provided.
Q17	Please provide the issue number, if available, in Lee <i>et al.</i> (2018).	The issue number is not provided.
Q18	Please provide the issue number, if available, in Manjunath <i>et al.</i> (2020).	The issue number is not provided.
Q19	Please provide the issue number, if available, in Mathews <i>et al.</i> (2021).	The issue number is not provided.

Q20	Please check changes to reference MIT 2018 are OK	OK.
Q21	Please provide the issue number, if available, in Monosi <i>et al.</i> (2016).	The issue number is not provided.
Q22	Please provide the issue number, if available, in Rahal and Hassan (2021).	The issue number is not provided.
Q23	Please provide the issue number, if available, in Rahal <i>et al.</i> (2016).	The issue number is not provided.
Q24	Please provide the issue number, if available, in Revilla-Cuesta <i>et al.</i> (2022).	The issue number is not provided.
Q25	Please provide the issue number, if available, in Roslan <i>et al.</i> (2020).	The issue number is not provided.
Q26	Please provide the issue number, if available, in Ruiz (2021).	The issue number is not provided.
Q27	Please provide the issue number, if available, in Ruiz <i>et al.</i> (2015).	The issue number is not provided.
Q28	Please provide the issue number, if available, in Santamaría <i>et al.</i> (2017).	The issue number is not provided.
Q29	Please provide the issue number, if available, in Silva <i>et al.</i> (2015).	The issue number is not provided.
Q30	Please provide the issue number, if available, in Soetens and Matthys (2017).	The issue number is not provided.
Q31	Please provide the issue number, if available, in Waseem and Singh (2016).	The issue number is not provided.
Q32	Please provide surnames & initials of editors, publisher name, city/ town, state name (if USA), country in Yusuf <i>et al.</i> (2019)	Editors: Hadjisophocleous G., Johnson R. Publisher: N/A City: Ottawa, Ontario, Canada Date: 5-7 June 2019 - ISBN: 9781488400100
Q33	Please provide the issue number, if available, in Zanini (2019).	The issue number is not provided.
Q34	s.s.d. changed to saturated surface-dry: is this OK?	OK.
Q35	Table 2: SP changed to superplasticiser: is this OK?	OK.